Jour. Petrol. Soc. Korea
Vol. 3, No. 2, p. 109~127, 1994

Petrology and geochemistry of the Seoul granitic batholith

Kwon, S.T.[1] · Cho, D.L.[1] · Lan, C.Y.[2] · Shin, K.B.[1] · Lee, T.[2] and Mertzman, S.A.[3]

[1]Department of Geology, Yonsei University, Seoul, Korea.
[2]Institute of Earth Sciences, Academia Sinica, P.O. Box 1-55, Nankang, Taipei, Taiwan 115.
[3]Department of Geosciences, Franklin and Marshall College, Lancaster, Pennsylvania, 17604-3003 U.S.A.

ABSTRACT : We report field relationship, petrography and major and trace element chemistry for the central part of the Seoul granitic batholith of Jurassic age occurring in the Kyonggi massif. The batholith consists mainly of biotite granite (BG) and garnet biotite granite (GBG) with minor tonalite-quartz diorite and biotite granodiorite with or without hornblende. The mode data, along with those reported by Hong (1984) for the biotite granite (south-BG) in the southern part of the batholith, indicate that the many of BGs and majority of GBG and south-BG are leucocratic. Major element data indicate that these predominant rocks of the batholith are peraluminous. Variation trends in Harker diagrams for the major and trace elements suggest that the BG and GBG are not related by a simple crystal fractionation process. The same is true between the central (BG and GBG) and the southern (south-BG) parts of the batholith, suggesting that the central and southern parts of the Seoul batholith may consist of three seperate intrusions. Tectonic discriminations using major and trace element data and the age of emplacement suggest that the batholith represents Jurassic plutonism related to an orogeny, perhaps to a subduction-related continental magmatic arc.

Key words : Seoul batholith, geochemistry, peraluminous granite, tectonic setting, intrusion complex

INTRODUCTION

Peraluminous granite is defined by the alumina saturation index, i.e., molar $Al_2O_3/(CaO+Na_2O+K_2O)$ ratio [A/CNK], being greater than one (Shand, 1947). It incorporates a significant proportion of the granitoid rocks on the surface of the earth. It is characterized mineralogically by the presence of Al-rich phases such as muscovite, garnet, cordierite, or aluminosilicates.

Mesozoic granitoid rocks on the Korean peninsula have been studied extensively mainly due to their relationship with ore deposits. However, studies about peraluminous granite are rare, despite potentially signifcant distribution of this rock type in Mesozoic granites.

The Seoul granitic batholith, whose composition is mainly peraluminous, is one of the major plutonic bodies in the Kyonggi massif. The geology of the northern part of the Kyonggi massif is not well known. For example, no detailed geologic maps have been published for this part of the massif. However, recent interest in the tectonics of the Kyonggi massif (Cluzel *et al.*, 1990; Fitches *et al.*, 1991; Liu, 1993; Yin and Nie, 1993) has encouraged us to investigate the Seoul batholith. Our goal is to better understand the evolution of the Kyonggi massif, since peraluminous granites are known to be generally associated with continent-continent collision (e.g., Clarke, 1992).

In this study, we describe preliminary field relationship and detailed petrography for the central part (Uijongbu-Pochon area) of the Seoul granitic batholith, and present major and trace element data for biotite granites and garnet biotite granites which are predominant rock types in the study area. With these chemical data we discuss genetic relationships between different

rock types, and tectonic setting. Another purpose of this study is to promote study of peraluminous granite, which can contribute to a better understanding of the nature of Mesozoic plutonism on the Korean peninsula.

GEOLOGIC BACKGROUND

The Seoul batholith in the central part of the Korean Peninsula has not been mapped in detail. Only two published geologic maps are available for the southern part of the batholith. Figure 1 is a tentative, simplified geologic map of the Seoul batholith and its vicinity modified after GMIK (1 973). The inset of Fig. 1 shows distribution of Jurassic Daebo granites and Cretaceous Bulgugsa granites, which is a traditional classification of Mesozoic granites in South Korea. Recently, however, Triassic plutons were identified among the so-called Daebo granites (Choo and Kim, 1986).

The Seoul granitic batholith of Mesozoic age was intruded into Precambrian basement rocks of the Kyonggi massif. Although the batholith has rather irregular boundaries against the surrounding rocks, it has a general distribution trend of NNE direction as opposed to the NE trend of other important Mesozoic batholiths in South Korea. Several granitic stocks, such as the Kwanaksan granite and the Suwon granite which occur to the south of the batholith may well be its extension.

The lithology of the Seoul batholith has been known simply as biotite granite (GMIK, 1973). Hong (1984) presented petrography, and major and trace element chemistry for the southern part (between Uijongbu and Seoul) of the batholith. Hong (1984) concluded that the granites in this area belong to subsolvus biotite monzogranite.

An early attempt to measure the age of the batholith was made by Ueda (1969). Ueda reported a Rb-Sr age of 202+/−15 Ma, a K-Ar feldspar (K-feldspar?) age of 65 Ma for the granites in Bulamsan area and a Rb-Sr age of 165+/−30 Ma for the granite in Pochon area. However, it is not clear whether the Rb-Sr ages are from a whole rock isochron or not. Kim (1971) gave a K-Ar K-feldspar age of 157 Ma from a granite in Uijongbu area. No attempts were made to recalculate the above ages using new decay constants, since no information about decay constants used was reported. Park (1972) and Fullagar and Park (1975) reported Rb-Sr whole rock age of 158+/−1 Ma (recalculated with new decay constant of ^{87}Rb of Steiger and Jager (1977)) and initial Sr isotope ratio of 0.7116+/−0.0003 for the granites in the southern part of the batholith. These radiometric ages indicate that the central and southern parts of the Seoul batholith are of Jurassic age.

Precambrian rocks in the vicinity of the Seoul batholith consist of banded gneiss, porphyroblastic gneiss with or without garnet, and granitic gneiss belonging to the Shiung group of the Kyonggi metamorphic complex (Kim, 1973; Na, 1978). According to Na (1979), these rocks experienced amphibolite to granulite facies metamorphism of low pressure type. The reported Rb-Sr whole rock ages of Precamrian basement samples range from about 2.7 to 1.8 Ga; that is, late Archean to early Proterozoic (Na and Lee, 1973; Fullagar and Park, 1975; Choo and Kim, 1983). Although the meaning of these ages is not clear, they can serve as the minimum age of the analyzed rocks.

FIELD RELATION AND PETROGRAPHY

Granitic rocks in the study area can be divided into five rock types according to their mode and mafic mineral assemblages : biotite granite (BG), garnet biotite granite (GBG), quartz diorite-tonalite, hornblende biotite granodiorite and biotite granodiorite. The majority of rocks in the study area belongs to the first three rock types, while the last two types are minor. Although many BGs and GBGs contain muscovite, it is unclear whether the muscovite is primary or secondary. Therefore, we did not attempt any further classifi-

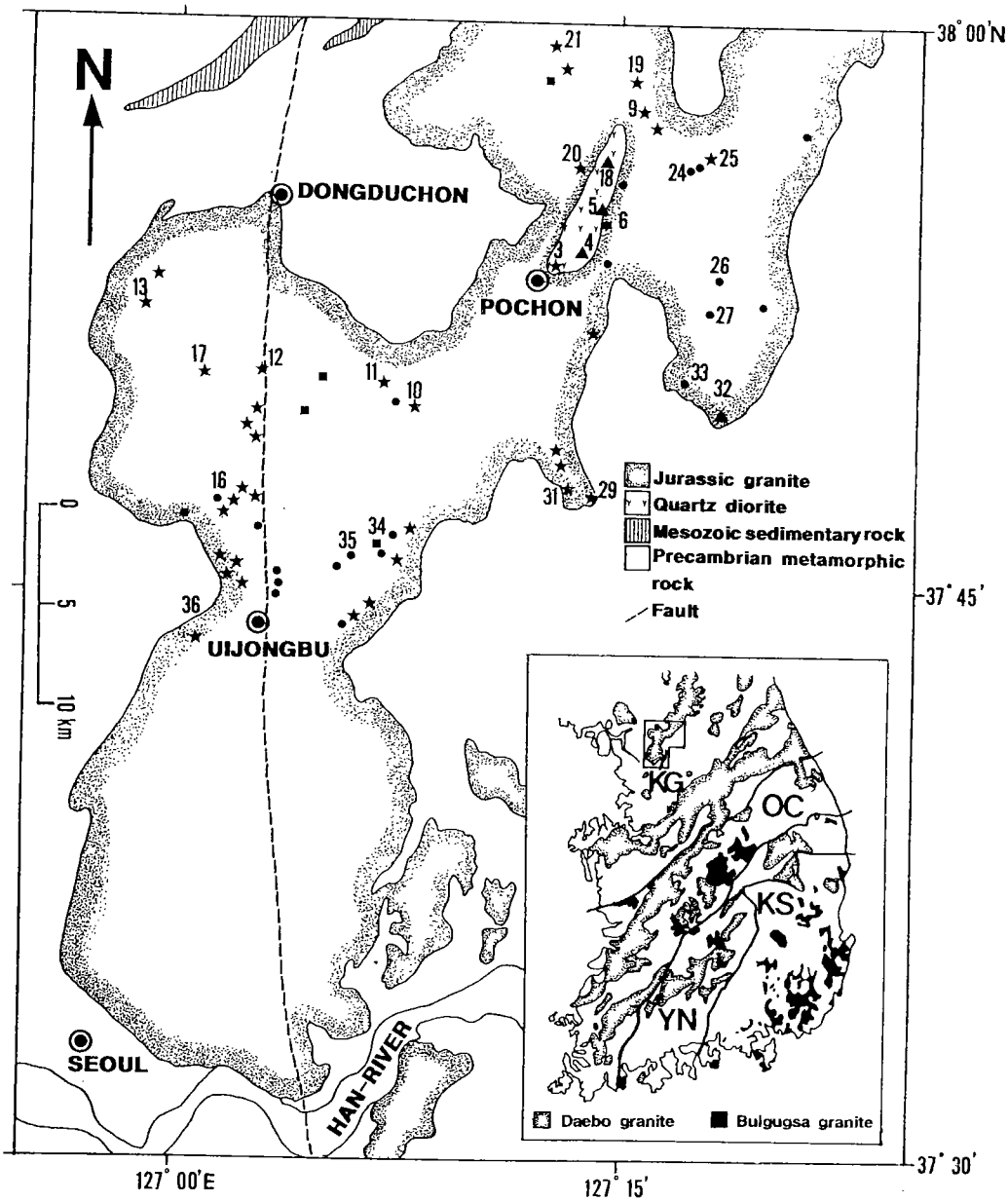

Fig. 1. Simplified geologic map and sample locations of the study area modified after GMIK (1973). Symbols : star, biotite granite; circle, garnet biotite granite; triangle, quartz diorite or tonalite. The inset shows distribution of Jurassic Daebo granite and Cretaceous Bulgugsa granite with tectonic provinces : KG, Kyonggi massif; OC, Ogcheon belt; YN, Youngnam massif; KS, Kyongsang basin.

cation based on the occurrence of muscovite.

Locations of samples analyzed for mode and/or chemistry are also shown in Fig. 1. Mode data are listed in Table 1 and are presented in modified classification diagrams (Fig. 2a and 2b) of plutonic rocks (Streckeisen, 1976). In Fig. 2a, most of rocks in the study area, together with biotite granites (south-BGs) of Hong (1984) from the southern

Table 1. Mode data for the Seoul granitic batholith in Uijongbu-Pochon area

Rock type	Sample	Qtz	Pl	Kfs	Cpx	Hbl	Bt	Ms	Chl	Ep	Grt	Aln	Ap	Zrn	Spn	Opq
BG	S3	20.5	40.2	30.4	-	-	7.0	1.1	0.7	tr	-	tr	tr	tr	0.1	tr
	S10	38.3	15.0	42.9	-	-	3.0	tr	0.6	-	-	0.1	tr	0.1	-	tr
	S11	27.9	31.8	34.5	-	-	4.4	0.2	1.1	-	-	-	tr	tr		tr
	S12	24.6	28.4	42.1		-	3.8	0.4	0.6	-	-	-	tr	0.1	-	tr
	S12'	43.9	25.8	26.2	-	-	3.8		0.4	-	-	-	tr	tr	-	tr
	S13	28.6	21.1	42.6	-	-	6.9	tr	0.8	tr	-	-	tr	tr	-	tr
	S17-1	32.1	31.6	27.8	-	-	8.0	tr	0.4	-	-	-	tr	0.2	-	tr
	S19	22.3	31.1	43.9	-	-	1.9	-	0.7	-	-	tr	tr	tr	-	0.1
	S20	30.4	33.0	31.2	-	-	5.2	tr	0.3	tr	-	-	tr	tr	-	tr
	S21	22.8	38.9	35.1	-	-	2.1	-	1.1	-	-	-	tr	tr	tr	tr
	S25	39.5	34.2	17.5	-	-	7.0	1.1	0.5	tr	-	-	tr	0.2	-	tr
	S29	22.6	38.9	24.7	-	-	13.2	-	0.1	-	-	tr	tr	tr	tr	0.4
	S31	30.8	44.1	14.0	-	-	9.7	-	1.3	-	-	tr	tr	tr	tr	tr
	S35-1	38.0	31.1	28.5	-	-	0.1	2.2	-		-	-	tr	tr	-	tr
	S36	36.1	31.7	31.6	-	-	0.2	0.2	0.2	tr	-	-	tr	tr	-	tr
GBG	S6	31.8	27.0	38.7	-	-	0.3	0.7	1.1	-	0.4	-	tr	tr	-	tr
	S16	33.3	29.5	32.1	-	-	1.5	1.2	0.6	-	1.8	-	tr	tr	-	tr
	S16'	48.0	22.4	26.7	-	-	1.7	0.2	0.7	-	0.3	-	tr	tr	-	tr
	S24	30.9	29.1	35.1	-	-	4.2	0.2	0.1	-	0.1	-	tr	0.3	-	tr
	S26	32.8	33.0	29.3	-	-	4.5	0.1	0.1	-	0.2	-	tr	tr	-	tr
	S33	34.4	30.4	30.7	-	-	2.1	1.5	0.4	-	0.6	-	tr	tr	-	-
HBG	S34	16.9	46.4	22.9	-	0.7	12.8	-	-	-	-	0.1	tr	tr	tr	0.1
QD-T	S4	14.8	43.1	2.7	1.1	10.2	11.5	2.6	12.0	0.4	-	-	0.4	0.2	0.9	0.2
	S5	14.1	47.8	0.6	0.8	14.0	20.9	-	0.6	-	-	-	0.2	tr	0.8	0.4
	S18	5.4	53.0	1.3	0.5	15.4	21.9	-	1.5	-	-	-	tr	0.2	tr	0.8
	S32-1	5.9	66.0	1.1	-	3.8	18.8	0.3	1.7	-	-	-	0.5	tr	0.8	1.2

Abbreviations for mineral names after Kretz (1983)

Rock type : BG, biotite granite; GBG, garnet biotite granite; HBG, hornblende biotite granite; QD-T, quartz diorite-tonalite.

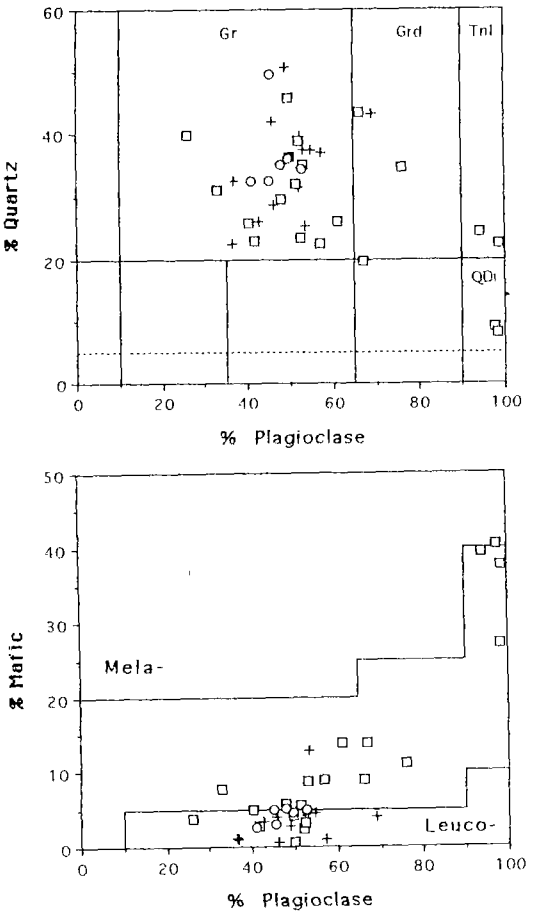

Fig. 2. Modified classification diagrams (Streckeisen, 1976) for granitic rocks without garnet (square) and with garnet (circle) from the central part of the Seoul batholith and for the biotite granites (cross) from the southern part reported by Hong (1984). Abbreviations : Gr, granite; Grd, granodiorite; Tnl, tonalite; QDi, quartz diorite.

part of the batholith, belong to granite, or to monzogranite with further classification based on alkali-feldspar/plagioclase ratio. Some belong to granodiorite, tonalite or quartz diorite. Fig. 2b classifies granitic rocks according to their mafic mineral contents. Some of BGs and all of GBGs belong to leucogranite. Note that most of south-BGs also belong to leucogranite. This indicates that a large part of the Seoul batholith are poor in mafic minerals.

Biotite granite is most abundant in the study area. Garnet biotite granite appears to crop out in two separate places, i.e., one to the north of Uijongbu city and the other to the east of Pochon city. The contact relationship between the biotite granite and garnet biotite granite is not certain. Inside the batholith, there is a small, mafic pluton elongated to the NNE-SSW direction just to the northeast of the Pochon city. This pluton consists mainly of quartz diorite and tonalite, and appears to have been intruded by a minor porphyritic granite (sample S3). Another quartz diorite (S32) was observed to the southeast of the Pochon city. Biotite granodiorite (S29 and S31) occurs as a small stock in the eastern part of the batholith. A hornblende biotite granodiorite (S34) was observed in the southern part of the study area. Cho and Kwon (1994) also reported a hornblende biotite granodiorite in the central part of the batholith.

Our preliminary results (Lan *et al.* in prep.) of whole rock Rb-Sr isotope dating indicate the following ages and Sr initial ratios : 156 Ma and 0.7135 for the biotite granite, 172 Ma and 0.7150 for the garnet biotite granite, and 325 Ma and 0.7108 for the quartz diorite-tonalite. This is the first time that the Paleozoic plutonism is reported in the Kyonggi massif.

Biotite Granite

Biotite granite is mostly medium- to coarse-grained. Major minerals are quartz, plagioclase, alkali feldspar and biotite. Accessary minerals are Fe-Ti oxides, allanite, apatite, sphene and zircon. Chlorite, epidote and muscovite occur as alteration products, although some muscovite appears to be of magmatic origin with subhedral form, well-terminated outline and size similar to that of biotite (Miller *et al.*, 1981). Quartz has subhedral form, and often occurs not only as anhedral aggregates but also as inclusions in alkali feldspar, biotite and plagioclase. Plagioclase occurs as subhedral to anhedral, platy crystals and often shows myrmekitic textures along the margin. Some pla-

gioclase have fine-grained biotite inclusions. When the plagioclase occurs as inclusions in alkali-feldspar, it usually shows resorbed texture. The alkali-feldspar is a subhedral perthitic microcline in most cases and it commonly includes other minerals. Biotite is subhedral and shows pleochroism of pale green to green, or of pale brown to yellow brown. Biotite has inclusions of apatite, opaque oxide minerals and zircon, and are associated with muscovite, allanite or sphene. Some of the biotite crystals are altered to chlorite. Epidote occurs as inclusions in altered plagioclase in most cases, suggesting a secondary origin.

Garnet biotite granite

Textures and phases of garnet biotite granite are similar to those of biotite granite except for the occurrence of garnet and lack of sphene. Some samples have no opaque oxides. Garnet occurs as euhedral inclusions in plagioclase or as independent grains with resorbed and subhedral form. Garnet is free of any inclusion. These features suggest that the garnet is of magmatic origin rather than derived from assimilation of country rocks (Allan and Clarke, 1981). Some garnet grains show faint optical zonation. Most muscovite is thought to be of secondary origin because its grain size is finer than that of biotite and by its occurrence as inclusions in altered biotite and plagioclase (Miller *et al.*, 1981). Some euhedral muscovite is in contact with biotite suggesting a magmatic origin.

Quartz Diorite-Tonalite

This rock is medium-grained and often contains plagioclase phenocrysts. Primary minerals include plagioclase, quartz, microcline, biotite, hornblende, clinopyroxene, apatite, zircon, sphene and opaque oxide, while the secondary minerals are chlorite, muscovite, sericite, epidote, and calcite. Plagioclase is predominantly subhedral and platy in form; it frequently shows optical zoning. Sometimes skeletal sphene with resorption texture is included in plagioclase. Phenocrystic plagioclase has fine-grained biotite, hornblende and quartz inclusions. Biotite is subhedral to anhedral and shows pale yellow-brown to reddish brown or dark brown pleochroism. Inclusions in biotite are commonly zircon, apatite and opaque oxide; rarely sphene, plagioclase or quartz. In some cases, biotite has cores of hornblende. Hornblende is closely associated with biotite, and often occurs as inclusions in plagioclase. Hornblende is subhedral or anhedral and shows pale brownish green to green pleochroism with patches of paler color. Hornblende often includes fine opaque oxide and quartz, and is partly altered to biotite. Clinopyroxene has hornblende rim and sometimes are replaced completely by fine-grained hornblende aggregates with relict pseudomorph. Microcline and quartz occur as interstitial minerals.

GEOCHEMISTRY

Concentrations of major and 14 trace elements (Rb, Ba, Sr, Zr, Y, Cr, V, Ni, Nb, Zn, Cu, U, Th, Ga) were obtained by X-ray fluorescence measurement utilizing a Philips PW-2400 vacuum spectrometer and using fused glass disks and pressed powder pellets respectively at the Department of Geology, Franklin and Marshall College, Lancaster, PA, U.S.A. Geochemical rock standards RGM-1 and JG-2 were prepared and analyzed as unknowns with the Seoul batholith samples. Based on these measurements, analytical uncertainties range from $<=1\%$ for major elements whose concentrations are $>10\%$ to approximately 5% for those major elements whose concentrations are $<1\%$. For 20 trace elements measured analytical uncertainties range from 1~2% at the 500 ppm concentration level to 10~15% at concentrations 20 ppm. The amount of ferrous Fe was titrated using a modified Reichen and Fahey method (1962). Concentrations of Be, Sc, Co, La, Ce and Yb were determined using an ICP-AES technique at the same institution. A detailed analytical pro-

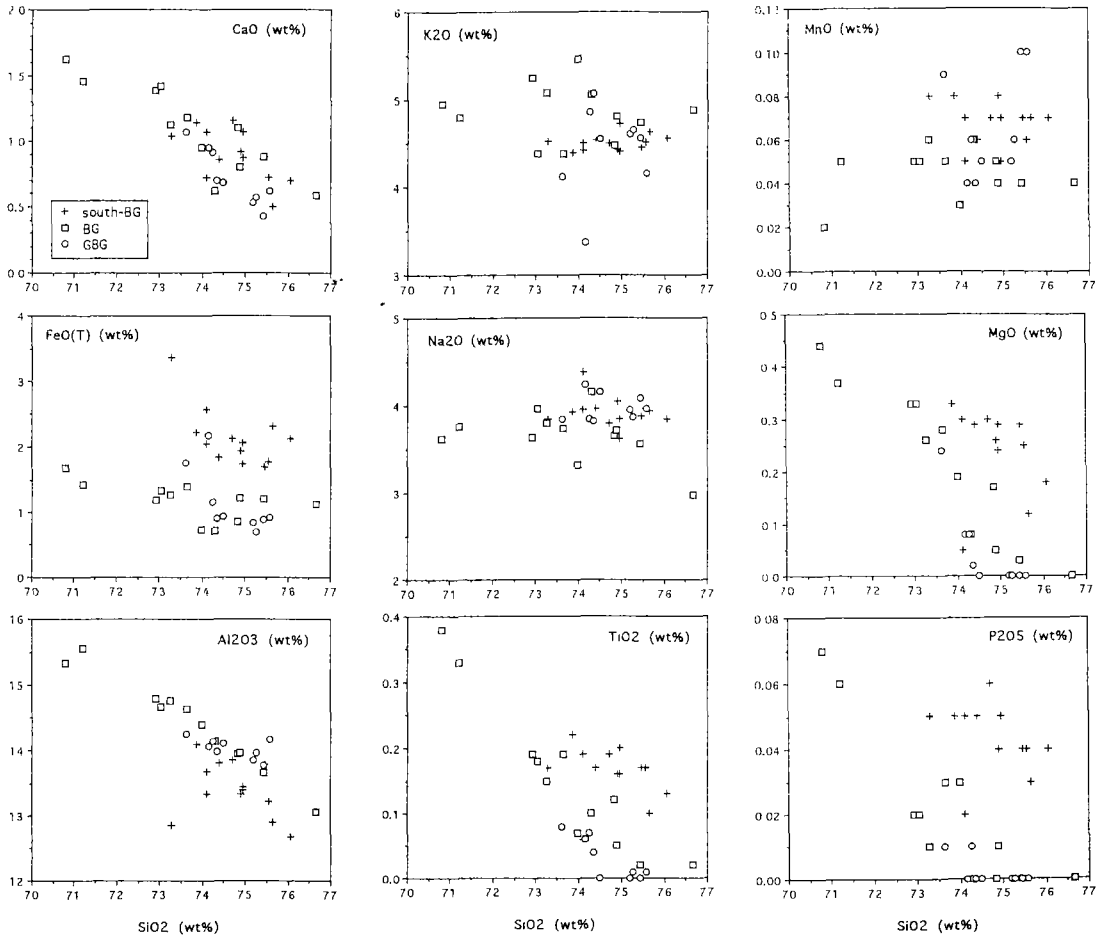

Fig. 3. Harker diagrams for major elemjents. Abbreviations : south-BG, biotite granite from the southern part of the Seoul batholith (Hong, 1984); BG, biotite granite; GBG, garnet biotite granite.

cedure appears in Boyd and Mertzman (1987).

Major and trace element data and calculated CIPW norm values for biotite granites and garnet biotite granites are given in Table 2. These data are discussed below, in comparison with those of biotite granites in the southern part of the batholith south of Uijongbu reported by Hong(1984).

Major elements

SiO_2 values of BG and GBG range from 70 to 77 wt %. GBG has more restricted values of 73 to 76 wt % which are similar to those of south-BG. Harker diagrams are shown in Fig. 3. In the diagrams, Al_2O_3, CaO, total FeO, MgO, TiO_2, and P_2O_5 show decreasing trends with increasing SiO_2, indicating fractionation of plagioclase, a mafic phase (probably biotite), titanomagnetite and apatite. Note, however, that CaO contents of GBG tend to have lower values than those of BG. The K_2O diagram depicts much scatter, while Na_2O contents are fairly constant at 3.5~4.2 wt %. The MnO diagram also shows scattered variation, with GBG showing tendency of higher values than BG. In Fig. 3, south-BG has higher MgO, total FeO, TiO_2, P_2O_5 and MnO contents and lower Al_2O_3 than BG and GBG, suggesting that they are not genetically related by crystal fractionation.

Most samples in the study area belong to peraluminous granite, as shown in A/NK (molar

Table 2. Major and trace element composition and CIPW norm of the Seoul batholith, Korea

Rock type	Biotite Granite												Garnet biotite granite								
Sample number	S9	S10	S11	S12	S13	S17	S17-1	S19	S20	S21	S25	S36	S6	S16	S16A	S16	S24	S26	S27	S33	S35
SiO_2(wt %)	76.66	75.42	74.87	73.65	70.80	73.05	71.21	73.25	72.92	74.82	73.98	74.30	74.50	75.58	74.14	75.27	73.62	74.26	74.34	75.44	75.18
TiO_2	0.02	0.02	0.05	0.19	0.38	0.18	0.33	0.15	0.19	0.12	0.07	0.10	0.00	0.01	0.06	0.01	0.08	0.07	0.04	0.00	0.00
Al_2O_3	13.06	13.67	13.97	14.63	15.33	14.67	15.55	14.76	14.80	13.96	14.40	14.14	14.11	14.18	14.06	13.97	14.26	14.14	13.98	13.77	13.85
Fe_2O_3	0.61	0.52	0.44	0.57	0.56	0.70	0.57	0.89	0.79	0.33	0.26	0.45	0.32	0.29	0.69	0.17	0.74	0.27	0.44	0.34	0.40
FeO	0.58	0.74	0.82	0.88	1.18	0.70	0.92	0.47	0.48	0.56	0.50	0.32	0.64	0.66	1.56	0.55	1.09	0.92	0.50	0.58	0.48
MnO	0.04	0.04	0.04	0.05	0.02	0.05	0.05	0.06	0.05	0.05	0.03	0.06	0.05	0.10	0.04	0.06	0.09	0.06	0.04	0.10	0.05
MgO	0.00	0.03	0.05	0.28	0.44	0.33	0.37	0.26	0.33	0.17	0.19	0.08	0.00	0.00	0.08	0.00	0.24	0.08	0.02	0.00	0.00
CaO	0.59	0.88	0.80	1.18	1.63	1.42	1.46	1.13	1.39	1.10	0.95	0.62	0.68	0.62	0.95	0.57	1.07	0.91	0.70	0.43	0.53
Na_2O	2.98	3.56	3.72	3.74	3.62	3.97	3.76	3.80	3.63	3.65	3.32	4.15	4.16	3.96	4.24	3.87	3.85	3.85	3.82	4.08	3.95
K_2O	4.88	4.74	4.81	4.38	4.95	4.38	4.80	5.08	5.25	4.48	5.46	5.06	4.55	4.15	3.37	4.66	4.12	4.86	5.07	4.56	4.61
P_2O_5	0.00	0.00	0.01	0.03	0.07	0.02	0.06	0.01	0.02	0.00	0.03	0.00	0.00	0.00	0.00	0.00	0.01	0.01	0.00	0.00	0.00
LOI	0.71	0.77	0.82	0.85	0.81	0.92	0.80	0.66	0.69	0.83	0.73	0.45	0.64	1.07	1.04	0.65	0.91	0.55	0.66	0.56	0.98
Total	100.13	100.39	100.40	100.43	99.79	100.39	99.88	100.52	100.54	100.07	99.92	99.73	99.65	100.62	100.23	99.78	100.08	99.98	99.61	99.86	100.03
Q(%)	39.13	34.22	32.57	31.87	26.36	29.51	27.13	28.94	28.32	33.56	31.26	29.30	31.00	34.83	33.41	33.28	32.21	30.58	30.95	32.91	33.15
C	1.81	1.09	1.22	1.67	1.22	0.87	1.66	0.98	0.67	1.11	1.38	0.71	1.11	2.05	1.71	1.53	1.55	0.92	0.94	1.34	1.40
Or	28.83	28.00	28.42	25.88	29.25	25.88	28.36	30.01	31.02	26.47	32.26	29.90	26.88	24.52	19.91	27.53	24.34	28.71	29.95	26.94	27.24
Ab	25.20	30.11	31.46	31.63	30.62	33.58	31.80	32.14	30.70	30.87	28.08	35.10	35.18	33.49	35.86	32.73	32.56	32.56	32.31	34.51	33.41
An	2.93	4.36	3.90	5.66	7.63	6.91	6.85	5.54	6.76	5.46	4.52	3.08	3.37	3.08	4.71	2.83	5.24	4.45	3.47	2.13	2.63
Hy	0.60	1.04	1.25	1.62	2.21	1.32	1.69	0.65	0.83	1.07	1.11	0.36	1.00	1.14	2.47	0.96	2.03	1.66	0.61	0.97	0.64
Mt	0.88	0.75	0.64	0.83	0.81	1.01	0.83	1.28	1.15	0.48	0.38	0.65	0.46	0.42	1.00	0.25	1.07	0.39	0.64	0.49	0.58
Hm	0.00	0.00	0.00	0.00	0.00	0.00	0.00	0.00	0.01	0.00	0.00	0.00	0.00	0.00	0.00	0.00	0.00	0.00	0.00	0.00	0.00
Il	0.04	0.04	0.09	0.36	0.72	0.34	0.63	0.28	0.36	0.23	0.13	0.19	0.00	0.02	0.11	0.02	0.15	0.13	0.08	0.00	0.00
Ap	0.00	0.00	0.02	0.07	0.17	0.05	0.14	0.02	0.05	0.00	0.07	0.00	0.00	0.00	0.00	0.00	0.02	0.02	0.00	0.00	0.00
Water	0.71	0.77	0.82	0.85	0.81	0.92	0.80	0.66	0.69	0.83	0.73	0.45	0.64	1.07	1.04	0.65	0.91	0.55	0.66	0.56	0.98
Total	100.13	100.39	100.40	100.43	99.79	100.39	99.88	100.52	100.54	100.07	99.92	99.73	99.65	100.62	100.23	99.78	100.08	99.98	99.61	99.86	100.03

Table 2. continued

Rock type	Biotite Granite												Garnet biotite granite								
Sample number	S9	S10	S11	S12	S13	S17	S17-1	S19	S20	S21	S25	S36	S6	S16	S16A	S16	S24	S26	S27	S33	S35
Rb(ppm)	139.0	167.0	167.0	205.0	176.0	176.0	184.0	153.0	157.0	158.0	283.0	203.0	218.0	214.0	246.0	221.0	215.0	219.0	197.0	223.0	218.0
Ba	882.0	356.0	311.0	794.0	1229.0	797.0	895.0	894.0	860.0	621.0	569.0	163.0	5.0	1.3	336.0	110.0	303.0	302.0	266.0	12.0	27.0
Sr	131.0	90.0	77.0	229.0	416.0	249.0	314.0	183.0	238.0	150.0	148.0	27.0	6.0	23.0	82.0	24.0	80.0	71.0	60.0	11.0	10.0
Be	1.9	2.7	3.4	4.5	2.5	3.3	2.3	2.2	2.1	2.2	4.3	3.0	2.9	2.2	3.2	3.2	3.6	3.2	2.4	3.1	2.2
Ga	13.5	13.4	15.9	20.0	22.0	19.2	20.1	17.0	17.7	16.5	16.2	18.2	18.0	18.6	22.1	16.8	18.6	17.2	15.9	17.6	18.1
Cr	<1	<1	2.0	4.0	8.0	<1	<1	<1	1.0	2.0	6.0	<1	1.0	4.0	6.0	3.0	2.0	5.0	1.0	5.0	8.0
V	<1	2.0	4.0	8.0	14.0	10.0	12.0	9.0	14.0	7.0	8.0	2.0	1.0	1.0	6.0	1.0	11.0	4.0	3.0	<1	<1
Sc	2.0	2.4	3.1	2.6	2.2	2.5	2.5	2.2	2.1	2.0	2.3	3.9	3.2	3.2	3.2	3.0	5.2	3.7	2.8	3.5	2.9
Cu	<1	2.0	3.0	3.0	1.0	3.0	2.0	2.0	1.0	0.8	0.9	<0.5	<0.5	3.0	<0.5	8.0	3.0	1.0	0.5	<0.5	19.0
Zn	27.0	28.0	20.0	49.0	57.0	46.0	44.0	31.0	30.0	21.0	25.0	33.0	33.0	27.0	49.0	20.0	61.0	28.0	29.0	30.0	20.0
Ni	<1	<1	1.0	2.0	2.0	2.0	<1	1.0	1.0	1.0	2.0	1.0	<1	1.0	2.0	3.0	2.0	1.0	4.0	<1	2.0
Co	0.6	1.0	0.9	1.2	2.3	1.7	1.3	1.2	1.9	1.2	1.2	0.5	0.3	0.2	0.0	<0.1	0.9	0.9	0.8	0.2	<0.1
Zr	60.0	88.0	103.0	150.0	243.0	142.0	209.0	145.0	120.0	97.0	64.0	118.0	63.0	69.0	96.0	65.0	111.0	95.0	100.0	68.0	72.0
Nb	10.5	12.0	13.0	13.0	10.6	12.4	14.4	11.3	11.7	11.2	9.3	16.1	18.2	17.2	22.4	16.8	23.4	17.2	12.3	17.5	15.6
Y	9.0	13.0	16.0	13.0	7.0	13.0	11.0	8.0	9.0	5.0	9.0	22.0	28.0	27.0	22.0	21.0	70.0	26.0	19.0	32.0	21.0
U	1.0	2.7	3.4	7.7	3.7	5.2	3.5	2.1	2.5	4.0	2.6	5.5	3.8	10.0	7.0	7.8	5.1	4.5	3.0	2.6	5.2
Th	9.0	27.0	28.0	19.0	23.0	21.0	20.0	10.2	9.8	15.0	6.3	25.0	15.0	18.5	18.0	12.3	29.0	19.0	19.0	16.0	14.5
La	25.0	32.0	26.0	47.0	67.0	38.0	59.0	43.0	29.0	26.0	14.0	27.0	12.0	15.0	30.0	14.0	35.0	27.0	26.0	12.0	12.0
Ce	42.0	56.0	50.0	83.0	118.0	69.0	102.0	71.0	49.0	44.0	26.0	56.0	28.0	32.0	57.0	26.0	60.0	50.0	50.0	30.0	26.0
Yb	0.9	1.1	1.6	1.3	0.3	1.2	0.6	1.1	0.9	0.6	0.7	1.8	2.3	2.6	1.7	1.5	5.4	2.1	1.7	2.8	1.7

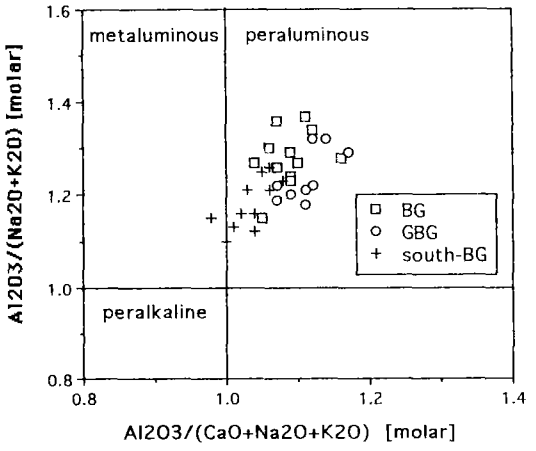

Fig. 4. Molar $Al_2O_3/(CaO+Na_2O+K_2O)$ [A/CNK] vs. $Al_2O_3/(Na_2O+K_2O)$ [A/NK] diagram. Symbols are the same as in Fig. 3.

($Al_2O_3/(Na_2O+K_2O)$) -A/CNK diagram (Fig. 4) and by the presence of corundum in CIPW norm (Table 2). Alumina saturation indices for most BGs and GBGs are greater than 1.05, which is typical of S-type granite proposed by White and Chappell (1983). In Fig. 4, the two variables show a fair, positive correlation together with the data for south-BG. GBGs tend to have lower A/NK values than BG for given A/CNK values, which is mainly due to slightly lower CaO and higher Na_2O contents of GBG compared with those of BG.

The characteristic major element variations shown by BG, GBG and south-BG suggest that the origin of BG and GBG could be different from that of south-BG, while the origin of GBG might not be simply related to fractional crystallization of BG.

Hong (1984) estimated the emplacement pressure of south-BG to be 1~2 kbar, using normative quartz-albite-orthoclase diagram of Tuttle and Bowen (1958). Although the leucocratic nature of the analyzed samples may approximate the ideal granitic system, the method should be used with great care. For example, it is well known that anorthite and fluorine components can shift the minimum composition of the Ternary system significantly (James and Hamilton, 1969; Manning and Pichavant, 1983).

Trace elements

Trace element variations are also shown in Harker diagrams (Figs. 5, 6 and 7). Figure 5 shows variaiton of Rb, Sr, Ba, Be, and Ga. Sr, Ba and Ga decrease with increasing SiO_2, suggesting fractionation of feldspars in agreement with major element data. GBG tends to have lower Sr and Ba , but higher Ga contents for given SiO_2 compared with BG. Sr data for south-BG plot along the BG trend. Rb contents of BG are relatively uniform except for one sample, and those of GBG have higher values than BG. Be contents vary between 2 and 4.5 ppm and do not show correlation with SiO_2.

Concentration of transition metals are generally low (Fig. 6), as can be expected for highly differentiated rocks of the study area. Ni, Co , V, Cr and Sc contents are less than 4 ppm, 2.3 ppm, 14 ppm, 8 ppm and 5.5 ppm, respectively. Nevertheless, they show some distinctions between BG and GBG. Co decreases with increasing SiO_2, and GBG tends to have lower Co content than BG. Sc contents of GBG tend to be higher than those of BG. V shows negative correlation with SiO_2, which includes data for south-BG. Cr shows no trend with SiO_2. However, south-BG have above 10 ppm and are clearly different from the BG and GBG. Zn contents vary between 20~60 ppm. Although Zn in general shows negative correlation with SiO_2, BG and GBG appear to follow differing variation trends. Cu contents are less than 4 ppm for BG and are variable between 1 and 20 ppm for GBG (not shown).

The variation of high field strength elements are shown in Fig. 7. Contents of Zr, and light rare earth elements (La and Ce) show decreasing variation with increasing SiO_2. Zr variation indicates fractionation of zircon, while La and Ce indicate fractionation of LREE-enriched phases such as apatite, allanite or monazite. GBG tends to have lower Zr contents compared with BG for given SiO_2 range. U and Th show scattered variation with SiO_2. Nb contents of BG are more or less

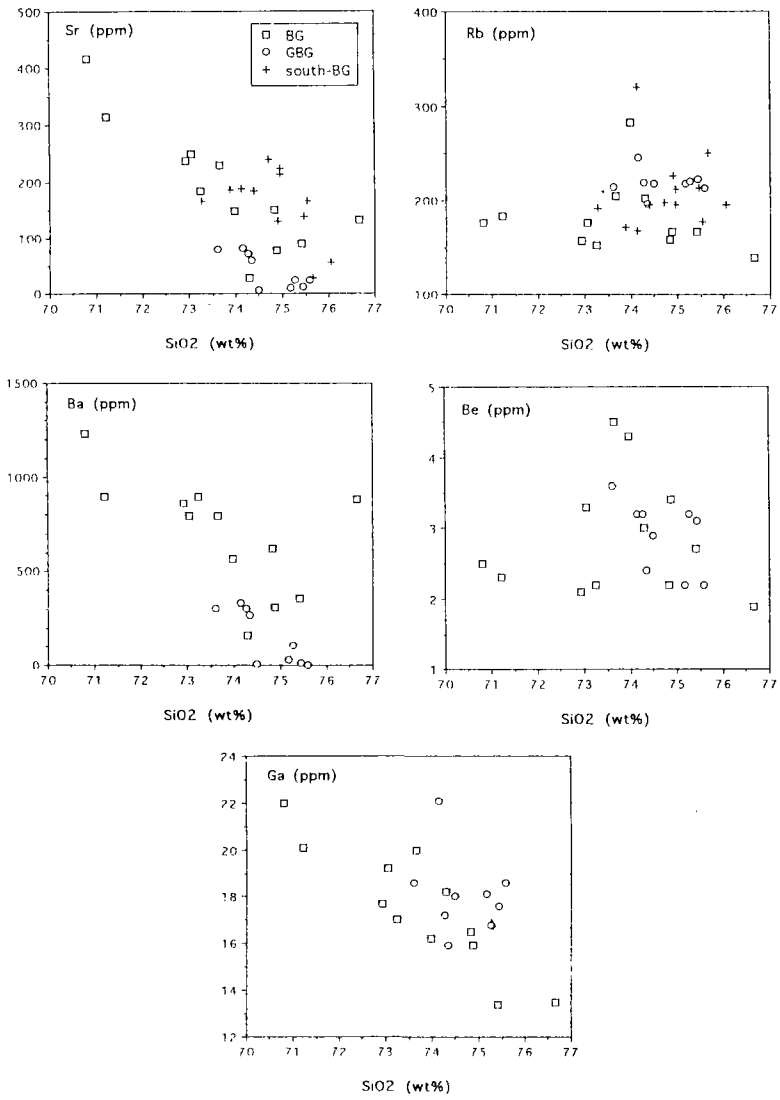

Fig. 5. Harker diagrams for Sr, Rb, Ba, Be and Ga. Symbols are the same as in Fig. 3.

uniform and are lower than those of GBG and south-BG, which is similar to the Rb-SiO_2 diagram. Y and Yb, having affinities with garnet, tend to be higher in GBG than in BG.

Trace element ratios : Nb/Zr, Rb/Zr, K/Rb, La/Yb and Y/Nb

Variation of trace element ratios are also shown in Harker diagrams (Fig. 8). The SiO_2-Nb/Zr diagram depicts a clear distinction between BG and other rocks. BG defines a well correlated increase in Nb/Zr ratio with SiO_2, while GBG and south-BG define steeper slopes, albeit scattered, than BG, probably indicating different origins. Similar features are observed in the Rb/Zr diagram except for one BG sample. The SiO_2-La/Yb diagram is shown in logarithmic scale. The La/Yb ratios of GBG are distinctly lower than those of BG, indicating that GBG has less LREE-enriched pat-

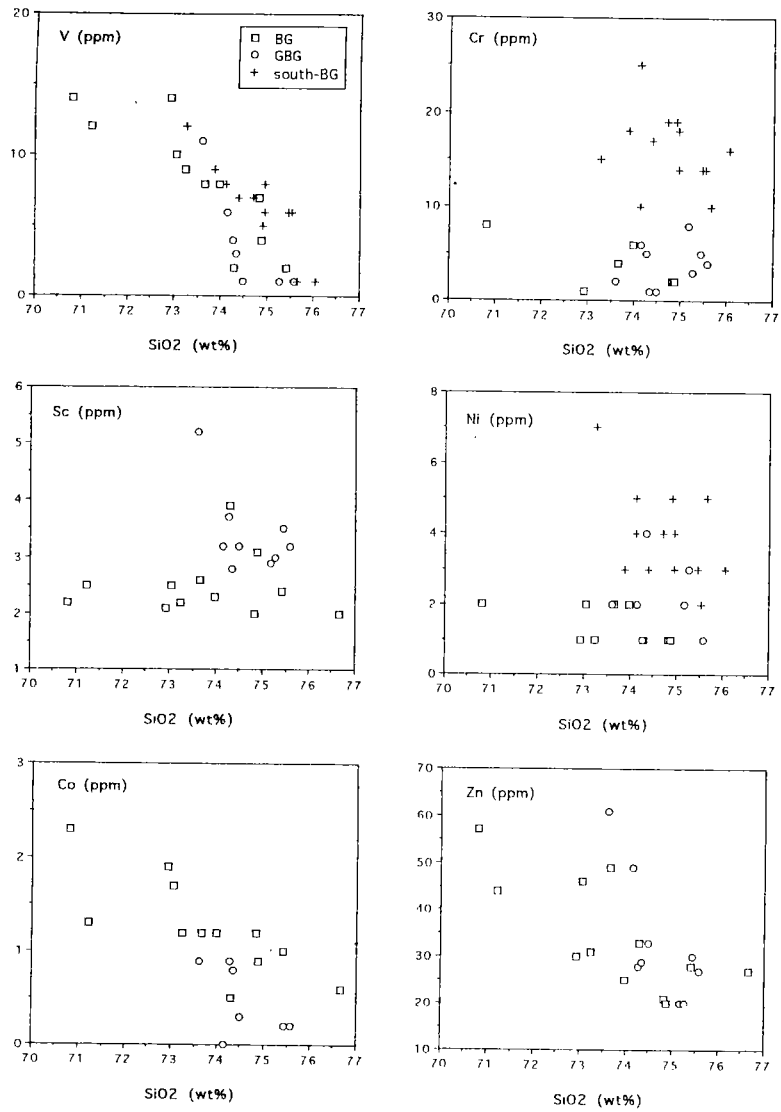

Fig. 6. Harker diagrams for transition elements. Symbols are the same as in Fig. 3.

tern compared with BG. This diagram shows that REE patterns have no relationship with SiO_2, i.e., with degree of fractionation. As would be expected, a reverse pattern to the La/Yb diagram exists in the SiO_2-Y/Nb diagram. The distinction between BG and other rocks also appear in K/Rb diagram, although less pronounced. In these trace element ratio diagrams, GBG appears to be similar to south-BG rather than BG.

Tectonic Setting

There have been several attempts to discrimi nate the tectonic setting of granitoid rocks using major and trace elements (Maniar and Piccoli, 1989; Pearce *et al.*, 1984; Harris *et al.*, 1986). Although these attempts are statistical in nature, they can provide some ideas about tectonic setting for the emplacement of granitoids. Major element

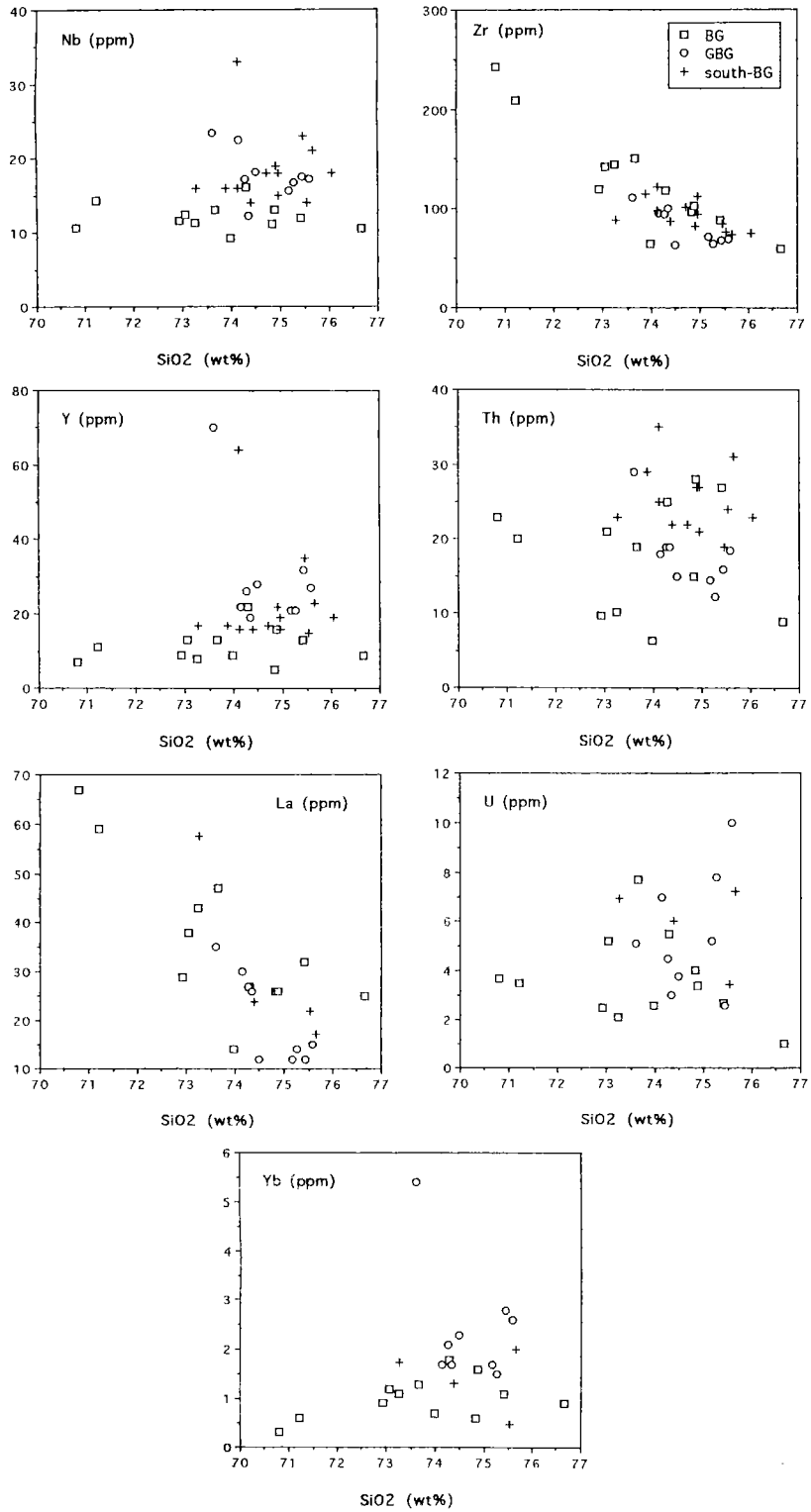

Fig. 7. Harker diagrams for high field strength elements. Symbols are the same as in Fig. 3.

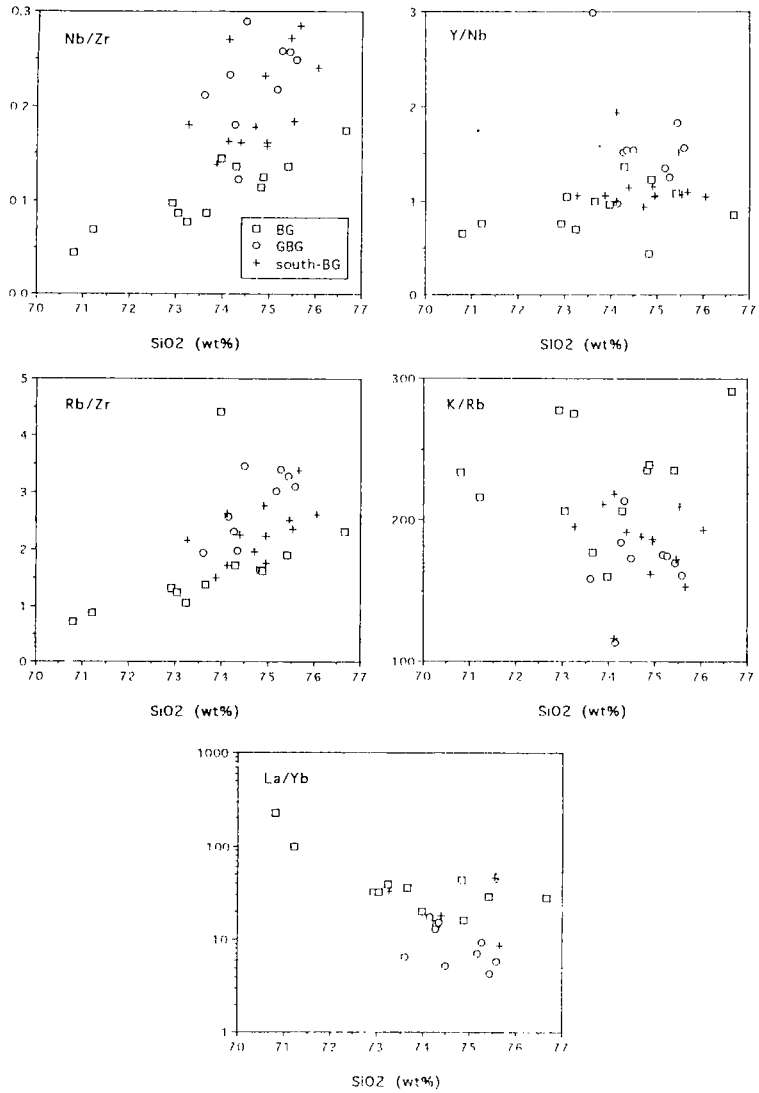

Fig. 8. Harker diagrams for trace element ratios. Symbols are the same as in Fig. 3.

discrimination diagrams of Maniar and Piccoli (1989) are shown in Fig. 9. They divided the tectonic settings of granitoids into four orogenic ones; island arc granitoids (IAG), continental arc granitoids (CAG), continental collision granitoids (CCG) and post-orogenic granitoids (POG), and three anorogenic ones; rift-related granitoids (RRG), continental epeirogenic uplift granitoids (CEUG) and oceanic plagiogranites (OP). Because the K_2O content of all samples is greater than 1 wt %, the Seoul batholith does not belong to OP. The four diagrams, i.e., SiO_2 vs. Al_2O_3, MgO vs. FeO (T), SiO_2 vs. FeO (T)/FeO (T)+MgO, and CaO vs. FeO (T)+MgO divide non-OP granitoids into three different groups : RRG+CEUP, IAG+CAG +CCG and POG. The variables of FeO (T), MgO, and CaO are not face values of data but modified ones. The definitions of these variables can be found in Maniar and Piccoli (1989). In these diagrams, BG and GBG appear to belong to IAG+ CAG+CCG group, and south-BG to POG. This suggests that the central part of the batholith

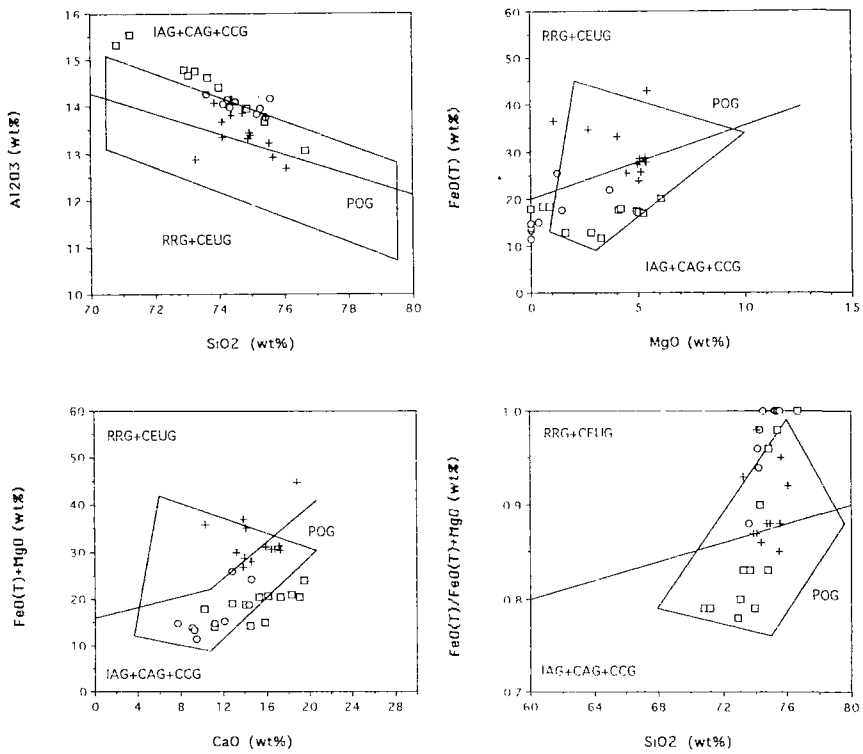

Fig. 9. Tectonic discrimination diagrams of Maniar and Piccoli (1989). Abbreviations : island arc granitoids (IAG), continental arc granitoids (CAG), continental collision granitoids (RRG), continental epeirogenic uplift granitoids (CEUG) and oceanic plagiogranites (OP). Symbols are the same as in Fig. 3.

might have formed in different tectonic setting from the southern part. However, if all the data are taken together, they can be interpreted as belonging to the IAG+CAG+CCG group. The present data do not allow further division of the IAG+CAG+CCG group using alumina saturation index (Maniar and Piccoli, 1989) since the majority of BG and GBG have alumica index of 1.05 ~1.15 which corresponds to the overlapping field for the three tectonic settings.

Tectonic discrimination using Y+Nb vs. Rb diagram of Pearce *et al.* (1984) is shown in Fig. 10. The majority of the samples, regardless of lithology, plot in the field of volcanic arc granites (VAG), but close to the boundary between VAG and syn-collisional granites (syn-COLG). In this diagram, VAG can be considered as combination of IAG and CAG, while syn-COLG as equivalent to CCG of Maniar and Piccoli (1989). Note, however, that the field for post orogenic granites overlap with those for VAG and syn-COLG (Pearce *et al.*, 1984). One way to discriminate VAG, syn-COLG and POG is using Rb/30−Hf−Ta×3 triangular diagram of Harris *et al.* (1986). Although the number of data for this plot is limited to four south-BGs reported by Hong (1984), three samples plot near the boundary between syn-COLG and POG field, and one to VAG field (not shown). Since these four samples plot within the field of VAG in the (Y+Nb) vs. Rb diagram, two discrimination schemes appear contradictory to each other. A similar circumstance is encountered when the four samples above are plotted in Yb-Ta diagram of Pearce *et al.* (1984), where three samples plot in syn-COLG and one to VAG (not shown). Although the appraisal of this problem

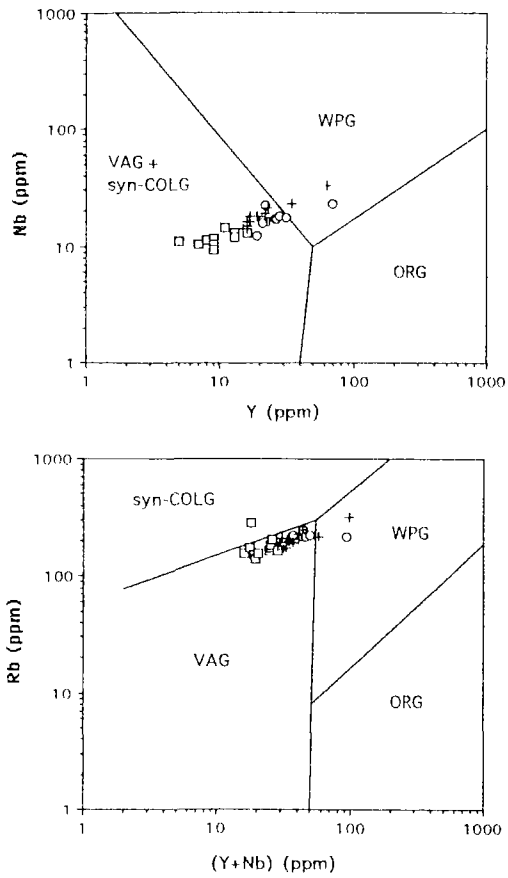

Fig. 10. Tectonic discrimination diagrams of Maniar and Piccoli (1989). Abbreviations : island arc granitoids (IAG), continental arc granitoids (CAG), continental collision granitoids (CCG), post-orogenic granitoids (POG), rift-related granitoids (RRG), continental epeirogenic uplift granitoids (CEUG) and oceanic plagiogranites (OP). Symbols are the same as in Fig. 3.

awaits Hf and Ta data for the same samples, we tentatively assign the tectonic setting of the Seoul batholith to VAG.

In summary, when major and trace element discrimination diagrams are taken together, the central and the southern parts of the Seoul batholith belong to orogenic granites. Among orogenic settings, IAG may be excluded from the geologic history of the Kyonggi massif during the emplacement of the batholith in Jurassic time, especially the existence of Precambrian basement rocks. However, further classification among CAG, CCG or POG requires more trace element data, or perhaps a better discriminant scheme, and more importantly better understanding of the tectonic history of the Kyonggi massif.

DISCUSSION AND CONCLUSION

Garnet biotite granite, first described in this study, is typically a peraluminous granite. Peraluminous granite is generally thought to be derived from pre-existing crustal rocks of sedimentary origin (Chappell and White, 1974) and to be associated with continent-continent collision tectonics (Clarke, 1992). However, it can also occur in association with subduction-related continental arcs (e.g., Ague and Brimhall, 1988), especially where old basement rocks exist. Although the granites in northern part of the Kyonggi massif have not been studied in detail, there are several other occurrences of garnet-bearing granite in the Kyonggi massif. The Kwanaksan granitic stock, to the south of the Seoul batholith, has garnet-bearing granite (Kwon *et al.*, unpublished data). Sim (1990) reported garnet two-mica granite in Kanghwa Island to the west of the Seoul batholith. Park *et al.* (1974) reported garnet-bearing granite to the north of Chunchon. These garnet-bearing granites occur in the northern part of the Kyonggi massif which is close to the Imjingang belt assumed to be a Triassic suture zone (Cluzel *et al.*, 1990; Liu, 1993; Yin and Nie, 1993). Although the geography of these peraluminous granites suggests a connection to collisional setting, the Jurassic age of emplacement for the Seoul batholith and perhaps for others indicate post-collisional, or newly-developed Jurassic continental arc magmatism. Tectonic discrimination using chemical data tentatively supports the latter option.

Major and trace element chemistries suggest that the central part of the Seoul granitic batholith might have a different origin from the southern part. Furthermore, in the central part, garnet biotite granites do not appear to be simply related by fractional crystallization from the biotite gra-

nites. These observations are supported by our preliminary Rb-Sr isotope data that indicate different ages and initial Sr isotopic ratios for central biotite granite and garnet biotite granite, and southern biotite granite. Although we have shown that the central and southern part of the Seoul batholith consists mainly of biotite granite and garnet biotite granite plutons with distinct origins, the question of how these intrusions and spatially associated minor stocks such as quartz diorite and granodiorite are related temporally and genetically remains to be investigated. Further studies including more REE data, isotope geochemistry and geochronology are neccessory to understand the origin of the Seoul batholith.

ACKNOWLEDGEMENTS

This study was sponsored by research grant 93-117 from Yonsei university and partially by a grant from CMR to S.T. Kwon, and in part by a grant NSC82-0202-M001-106 from the National Science Council of the Republic of China to C.Y. Lan. Constructive reviews by M. Cho, J.I. Lee and Y.K. Hong are greatly appreciated.

REFERENCES

Ague, J.J. and Brimhall, G.H., 1988, Regional variations in bulk chemistry, mineralogy and the compositions of mafic and accessory minerals in the batholiths of California. Geol. Soc. Am. Bull., 100, 891-911.

Allan, B.D. and Clarke, D.B., 1981 Occurrence and origin of garnets in the South Mountain batholith, Nova Scotia. Can. Mineral., 19, 19-24.

Boyd, F.R. and Mertzman, S.A., 1987, Composition and structure of the Kaapvaal lithosphere, southern Africa : In Mysen, B.O. (ed.), Magmatic processes : Physicochemical principles, Geochem. Soc. Spe. Publ., 1, 13-24.

Chappell, B.W. and White, A.J.R., 1974, Two contrasting granite types. Pacific Geol., 8, 173-174.

Cho, D.L. and Kwon, S.T., 1994, Hornblende geobarometry of the Mesozoic granitoids in South Korea and the evolution of crustal thickness. Jour. Geol. Soc. Korea, 30, 41-61. (in Korean)

Choo, S.H. and Kim, D.H., 1983, Rb/Sr age dating of the Gyeonggi gneiss complex in Anyang, Gapyeong, Yangsuri and Yongduri areas. Research report 82-1-16, Korea Inst. Energy and Resources, 79-102. (in Korean)

Choo, S.H. and Kim, S.J., 1986, Rb-Sr age determinations on the Ryeongnam massif (II) : Granitic gneisses and gneissose granites in the southwestern Jirisan region. Research report KR-86-7, Korea Inst. Energy and Resources, 7-33. (in Korean)

Clarke, D.B., 1992, Granitoid Rocks. Chapman and Hall, 283p.

Cluzel, D., Cadet, J.P. and Lapierre, H., 1990, Geodynamics of the Ogcheon belt (South Korea). Tectonophys., 183, 41-56.

Fitches, W.R., Fletcher, C.J.N. and Xu, J., 1991, Geotectonic relationships between cratonic blocks in E. China and Korea., Jour. Southeast Asian Earth Sci., 6, 185-199.

Fullagar, P.D. and Park, B.K., 1975, Rb-Sr study of granite and gneiss from Seoul, South Korea. Geol. Soc. Am. Bull., 86, 1579-1580.

GMIK (Geol. Min. Inst. Korea), 1973, 1 : 250,000 geological map of Korea. GMIK, Seoul, Korea.

Harris, N.B.W., Pearce, J.A. and Tindle, A.G., 1986, Geochemical characteristics of collision-zone magmatism. In : Coward, M.P. and Reis A.C. (eds.), Collision tectonics. Spec. Publ. Geol. Soc., 19, 67-81.

Hong, Y.K., 1984, Petrology and geochemistry of Jurassic Seoul and Anyang Granites, Korea. J. Geol. Soc. Korea, 20, 51-71.

James, R.S. and Hamilton, D.L., 1969, Phase relations in the system $NaAlSi_3O_8$-$KAlSi_3O_8$-$CaAl_2Si_3O_8$-SiO_2 at 1 kilobar water vapour pressure. Contrib. Mineral. Petrol., 21, 111-141.

Kim, O.J., 1971, Study on the intrusion epochs of younger granites and their bearing to orogenies in South Korea. J. Korea Inst. Mining Geol., 4, 1-9. (in Korean)

Kim, O.J., 1973, The stratigraphy and geologic structure of the metamorphic complex in the northwestern area of the Kyonggi massif. J. Korea Inst. Mine. Geol., 6, 201-218. (in Korean)

Kretz, R., 1983, Symbols for rock-forming minerals. Am. Mineral., 68, 277-279.

Liu, X., 1993, High-P metamorphic belt in central China and its possible eastward extension to Korea. Jour. Petrol. Soc. Korea, 2, 9-18.

Maniar, P.D. and Piccoli, P.M., 1989, Tectonic discrimination of granitoids. Geol. Soc. Am. Bull., 101, 635-643.

Manning, D.A.C. and Pichavant, M., 1983, The role of fluorine and boron in the generation of granitic melts. In, Atherton, M.P. and Gribble, C.D. (eds), Migmatites, Melting and Metamorphism, Shiva, Cheshire, 94-109.

Miller, C.F., Stoddard, E.F., Bradfish, L.J. and Dollase, W.A., 1981, Composition of plutonic muscovite : genetic implications. Can. Mineral., 19, 25-34.

Na, K.C., 1978, Regional metamorphism in the Gyeonggi Massif with comparative studies on the Yeoncheon and Ogcheon metamorphic belts (I). J. Geol. Soc. Korea, 14, 195-211.

Na, K.C., 1979, Regional metamorphism in the Gyeonggi Massif with comparative studies on the Yeoncheon and Ogcheon metamorphic belts (II). J. Geol. Soc. Korea, 15, 67-88.

Na, K.C. and Lee, D.J., 1973, Preliminary age study of the Gyeonggi metamorphic belt by the Rb-Sr whole rock method. J. Geol. Soc. Korea, 9, 168-174.

Park, B.K., 1972, Whole-rock rubidium-strontium age of the Seoul granite. J. Geol. Soc. Korea, 8, 156 -161.

Park, H.I., Chi, J.M., Chang, K.H. and Ko, I.S., 1974, Geologic map of Naepyeong sheet and explanatory text. Geological and Mineralogical Institute of Korea, 1-13.

Pearce, J.A., Harris, N.B.W. and Tindle, A.G., 1984, Trace element discrimination diagrams for the tectonic interpretation of granitic rocks. J. Petrol., 25, 956-983.

Reichen, L.E. and Fahey, J.J., 1962, An improved method for the determination of FeO in rocks and minerals including garnet. U.S. Geol. Surv. Bull., 144B, 1-5.

Shand, S.J., 1947, Eruptive rocks. Their Genesis, Composition, Classification, and their Relation to Ore-Deposits, 3rd ed., J. Wiley & Sons, New York, 488p.

Sim, W.J., 1990, Petrology of the granitic rocks in the southern Kanghwado Island and Seogmodo Island. unpublished M.S. thesis, Yonsei Univ., 60 p. (in Korean)

Steiger, R.H. and Jager, E., 1977, Subcommission on geochronolgy : Convention on the use of decay constants in geo- and cosmochronology. Earth Planet. Sci. Lett., 36, 359-362.

Streckeisen, A., 1976, To each plutonic rocks its proper name. Earth Sci. Rev., 12, 1-13.

Tuttle, O.F. and Bowen, N.L., 1958, The origin of granite in the light of experimental studies in the system $NaAlSi_3O_8$-$KAlSi_3O_8$-SiO_2-H_2O. Mem. Geol. Soc. Amer., No. 74, 153 p.

Ueda, N., 1969, Evolution of the continent in Northeastern Asia (I) : Reconaissance survey of the geochronology of the Korean Peninsula. J. Korea Inst. Mine. Geol., 2, 96-97. (in Korean)

White and Chappell, 1983, Granitoid types and their distribution in the Lachlan fold belt, southeastern Austrailia. In Roddick, J.A., ed., Circum-Pacific terranes. Geol. Soc. Am. Mem., 159, 21-34.

Yin, A. and Nie, S., 1993, An indentation model for the north and south China collision and the development of the Tan-Lu and Honam fault systems, eastern Asia. Tectonics, 12, 801-813.

(책임편집 : 좌용주)

서울 화강암질 저반의 암석학 및 지구화학

권성택[1] · 조등룡[1] · 籃晶瑩[2] · 신광복[1] · 李太楓[2] · 스탠리 머어츠먼[3]

[1]연세대학교 지질학과,

[2]대만 학술원 지구과학연구소,

[3]Department of Geosciences, Franklin and Marshall College, Lancaster, Pennsylvania, 17604-3003 U.S.A.

요 약 : 이 연구는 경기육괴의 서울 화강암질 저반(쥬라기)의 중앙부에 대한 야외관계, 암석기재, 주성분 및 미량성분 원소의 화학자료를 보고한다. 서울 저반은 주로 흑운모 화강암(BG)과 석류석 흑운모 화강암(GBG)으로 구성되며, 토날라이트-석영섬록암과 흑운모(+/-각섬석) 화강섬록암이 소규모로 산출한다. Hong(1984)이 보고한 서울 저반 남부지역의 흑운모 화강암(south-BG)과 같이 고려했을때, 모드 자료는 대부분의 GBG와 south-BG 그리고 많은 BG가 우백질에 속함을 지시한다. 주성분 원소는 이들 암석이 거의 모두 고알루미나질임을 나타낸다. 주성분 및 미량원소 성분은 하커 그림에서 BG와 GBG가 단순한 결정분별작용으로 설명될 수 없으며, 중부와 남부지역 암석 사이의 성인적인 관계도 마찬가지임을 나타낸다. 이는 서울 저반의 중부와 남부 지역은 3개의 서로 다른 관입체로 구성되었음을 시사한다. 화학자료를 이용한 지구조 판별과 정치시기는 서울 저반이 쥬라기의 조산운동과 관련된 심성활동이었음을 시사하는데, 특히 섭입과 관련된 대륙 마그마 호 환경이었을 것으로 추정된다.

핵심어 : 서울 저반, 지구화학, 고알루미나질 화강암, 지구조 환경, 관입복합체